ENGINEERING & TECHNOLOGY SCIENTIFIC JOURNAL

ORIGINAL

2023, VOL. 01, N°. 01, e023007
DOI: 10.55977/etsjournal.v01i01.e023007

Analysis of Spiral Plate Heat Exchanger Used to Cool Vegetable Oil with Nanofluid Consisting of Water and Non-Spherical Boehmite Alumina Nanoparticles

Élcio Nogueira [1*]

[1] Department of Mechanic and Energy, State University of Rio de Janeiro, Rio de Janeiro, Brazil.

Received 2022-10-20
Revised 2023-01-20
Accepted 2023-06-26
Published 2023-10-10

***Corresponding author**
Élcio Nogueira
elcionogueira@outlook.com

Page e-location ID
e023007

ABSTRACT

The objective is to use dimensionless analysis through the thermal efficiency method to determine the thermohydraulic performance of a spiral plate heat exchanger (S.P.H.E.) used to cool sunflower oil. The coolant consists of water as a base fluid and non-spherical Boehmite Alumina nanoparticles with a defined volume fraction. The concept of thermal efficiency for heat exchangers is used to determine the main quantities used in the analysis. Graphical results are presented for the number of thermal units (NTU), thermal efficiency, thermal effectiveness, hot fluid outlet temperature, thermal and viscous irreversibilities, and Bejan number. The analyzed heat exchanger provides excellent thermal performance for refrigerants consisting of water and non-spherical nanoparticles in platelets or cylindrical, with a volume fraction equal to 12.0%. Viscous dissipation significantly increases concerning the dissipation associated with pure water, but the cost-benefit is within reason for the proposed objective, within the flow rate under analysis.

Keywords Spiral Plate Heat Exchanger (S.P.H.E.); Thermal efficiency method; Vegetable oil; Nanofluid; Non-spherical shaped nanoparticles.

How to cite this article (APA): Nogueira, E. Analysis of Spiral Plate Heat Exchanger Used to Cool Vegetable Oil with Nanofluid Consisting of Water and Non-Spherical Boehmite Alumina Nanoparticles: *Engineering & Technology Scientific Journal, 01(01)*, e023007.

1. INTRODUCTION

The second law of thermodynamics is applied in spiral plate heat exchangers (S.P.H.E.), emphasizing the thermal efficiency of heat exchangers. It is an analytical solution for cooling vegetable oil using non-spherical alumina nanoparticles in the shape of platelets and cylindrical. The results for heat transfer coefficients, number of thermal units (NUT), thermal efficiency, thermal effectiveness, thermal and viscous irreversibilities, hot fluid outlet temperature, and Bejan number are obtained and presented graphically through thermo-hydrodynamic performance analysis.

Shirazi et al. (2022) present an exegetical analysis of spiral plate heat exchangers (S.P.H.E.s) using an algorithm that makes it possible to obtain a more compact and efficient S.P.H.E. Mathematical Modeling numbers based on dimensionless energy, in addition to thermal efficiency and temperature difference number and modified. These dimensionless numbers allow the evaluation of exergy in channels. Furthermore, the temperature distribution was validated with a computer simulation of fluid dynamics. The results show the most significant increase in the relative heat transfer rate by volume of S.P.H.E., up to 54%, compared to other projects.

Khorshidi & Heidari (2016) analyze the performance of a spiral plate heat exchanger. Using Fluent software, they design and build prototypes of galvanized iron sheets for analysis and comparison with the theoretical model. They claim that the spiral heat exchanger is an excellent alternative to other heat exchangers, especially for highly viscous fluids. In addition, the low fouling rate reduces the need for frequent cleaning.

Kolasiński & Rogala (2015) state that spiral plate heat exchangers are often used in domestic heating because of less material used and lower installation expense. What makes the spiral plate heat exchanger competitive is the relatively high heat transfer rate achieved. The complex mathematical analysis results show that the S.P.H.E. is effectively an interesting alternative to other types of heat exchangers due to the reduction in installation size and expenses.

Kumar et al. (2018) state that researchers are becoming more aware of using spiral heat exchangers for heat transfer. They describe the heat exchanger as formed by a sheet arrangement with two channels wound around each other, and the distance between the sheets is kept constant to keep the cross-sectional area along the flow path. They analyze the performance of S.P.H.E. in a counterflow type configuration. The results obtained make it possible to determine how to optimize the flow of fluids to increase the efficiency of the heat exchanger.

Núñez et al. (2007) present an alternative design approach for dimensioning single-phase counter-current spiral plate heat exchangers. The method used results in a design methodology that maximizes the pressure drop and results in the design of the most diminutive dimensions. In the counter-current arrangement, both fluids have the same flow length. The degree of freedom used in the design is the spacing of the plates which can be changed so that both flows maximize their allowable

pressure drop. The results obtained by the adopted approach are compared with the results of projects presented in the open literature and show that the method is reliable and easy to implement.

Hemanth et al. (2022) state that one way to increase the thermal heat performance in a spiral plate heat exchanger is to employ nanofluid. In this sense, they present a numerical analysis of the effects of nanofluids and validate them through experimental results in a counterflow heat exchanger. The nanoparticles used were titanium dioxide (TiO_2) and silicon dioxide (SiO_2) with water as the base fluid. The results obtained show a 20 to 25% increase in heat transfer at a volume concentration equal to 3%.

2. METODOLOGY

The S.P.H.E. is used to cool sunflower vegetable oil with an inlet temperature equal to 110 °C. The nanofluid, made up of water and nanoparticles in the form of platelets or cylinders, is the coolant. The inlet temperature of the refrigerant fluid is equal to 30 °C. The heat exchanger has a height of 1.2 meters, and the spiral has a length of 2,485 meters, with turns equal to 10. The inner diameter is equal to 0.1 meters, and the outer diameter is equal to 0.225 meters. The total heat exchange area is 6.0 m^2. The channel width is equal to 0.005 meters. The average temperature of the hot fluid is 55 °C.

Fig. 1 represents a spiral plate heat exchanger and its basic dimensions. **Fig. 2** schematically illustrates a counter-current heat exchanger of length L. **Tab. 1** presents the values of the basic properties of hot and cold fluids and Boehmite Alumina nanoparticles. **Tab. 2** shows coefficients that characterize the non-spherical nanoparticles in the shape of platelets and cylindrical.

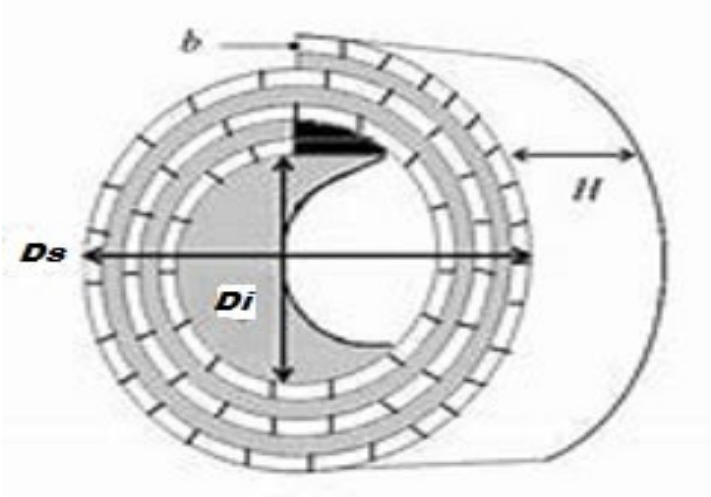

Figure 1. Spiral Plate Heat Exchanger (S.P.H.E.).
Source: (Kumar et al., 2018).

Table 1. Properties of cold fluid (water) and Boehmite Alumina nanoparticles.

	kg/m³	W/(m.K)	J/(Kg.K)	Kg/(m.s)
Cool	994.5	0.605	4182.5	$0.875\ 10^{-3}$
Alumina	3050	30	618.3	-

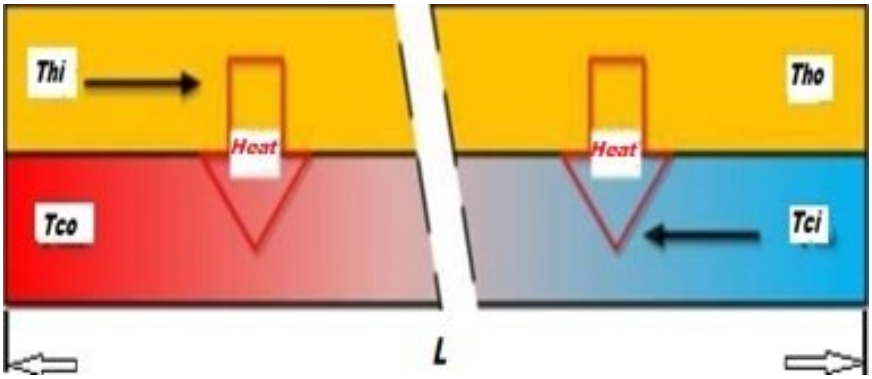

Figure 2. Schematic representation of Counter-Flow Heat Exchanger.
Source: (Núñez et al., 2007)

Table 2. Coefficients that characterize the non-spherical shape of nanoparticles in dynamic viscosity and thermal conductivity.

Type	C_k	A_{11}	A_{22}
Platelets	2.61	37.1	612.6
Cylindrical	3.95	13.5	904.4

$$L = 2.485m \quad \textbf{(Eq. 1)}$$
$$b_c = 0.005m \quad \textbf{(Eq. 2)}$$
$$b_h = 0.005m \quad \textbf{(Eq. 3)}$$
$$b = \frac{b_c + b_h}{2} \quad \textbf{(Eq. 4)}$$
$$H = 1.2m \quad \textbf{(Eq. 5)}$$

The properties of the cold fluid are obtained from the quantities represented in **Tab. 1.**

$$v_c = \frac{\mu_c}{\rho_c} \quad \textbf{(Eq. 6)}$$
$$\alpha_c = \frac{k_c}{\rho_c c p_c} \quad \textbf{(Eq. 7)}$$
$$Pr_c = \frac{v_c}{\alpha_c} \quad \textbf{(Eq. 8)}$$
$$Th_{Med} = 55.0\ °C \quad \textbf{(Eq. 9)}$$

The properties of the hot fluid are obtained through polynomial interpolation of the data given in Rojas et al. (2013):

$$\rho_h = 920.8893939 - 0.09046037296\,Th_{Med} - 0.0003712121212\,Th^2{}_{Med} + 2.33100233110^{-6}\,Th^3_{Med} \quad \textbf{(Eq. 10)}$$

$$\mu_h = 0.1446810076 - 0.00571479528Th_{Med} + 9.8117277110^{-5} + Th^2{}_{Med} - 7.88058566410^{-7}Th^3_{Med} + 2.40260780910^{-9}Th^4{}_{Med} \quad \textbf{(Eq. 11)}$$

$$k_h = 0.1595212121 + 7.62626262610^{-5}Th_{Med} - 5.30303030310^{-7}Th^2_{Med} + 2.52525252510^{-9}Th^3{}_{Med} \quad \textbf{(Eq. 12)}$$

$$Cp_h = 2046.651515 + 3.511130536Th_{Med} + 0.005606060606Th^2{}_{Med} + 9.90675990710^{-6}Th^3_{Med} \quad \textbf{(Eq. 13)}$$

$$v_h = \frac{\mu_h}{\rho_h} \quad \textbf{(Eq. 14)}$$

$$v_h = \frac{k_h}{\rho_h Cp_h} \quad \textbf{(Eq. 15)}$$

$$Pr_h = \frac{v_h}{\alpha_c} \quad \textbf{(Eq. 16)}$$

The properties of nanofluids are given by (Nogueira, 2020; Hemanth et al., 2022):

$$\rho_{nano} = \rho_{Particle}\phi + (1-\phi)\rho_C \quad \textbf{(Eq. 17)}$$

$$\mu_{nano} = \frac{\mu_C}{(1-\phi)^2} \quad \textbf{(Eq. 18)}$$

$$\mu_{nano} = \mu_C(1 + A_1\phi + A_2\phi^2)\; non - spherical\; shape \quad \textbf{(Eq. 19)}$$

$$Cp_{nano} = \frac{Cp_{particle}\,\rho_{Particle}\phi + (1-\phi)Cp_C\,\rho_C}{\rho_{nano}} \quad \textbf{(Eq. 20)}$$

$$k_{nano} = \left[\frac{[k_{particle} + 2k_C + 2(k_{particle} - k_C)(1-0.1)^3\phi]}{[k_{particle} + 2k_C + 2(k_{particle} - k_C)(1-0.1)^2\phi]}\right] K_C \quad \textbf{(Eq. 21)}$$

$$k_{nano} = k_C(1 + C_k\phi) forma\; não\; esférica \quad \textbf{(Eq. 22)}$$

$$v_{nano} = \frac{\mu_{nano}}{\rho_{nano}} \quad \textbf{(Eq. 23)}$$

$$\alpha_{nano} = \frac{k_{nano}}{\rho_{nano}\,Cp_{nano}} \quad \textbf{(Eq. 24)}$$

$$Pr_{nano} = \frac{\mu_{nano}}{\alpha_{nano}} \quad \textbf{(Eq. 25)}$$

ϕ is the volume fraction of the nanoparticles.

$$\gamma_{nano} = \rho_{nano} G \quad \text{(Eq. 26)}$$

$$\gamma_h = \rho_h G \quad \text{(Eq. 27)}$$

$$S_{nano} = \frac{\rho_{nano}}{\rho_c} \quad \text{(Eq. 28)}$$

$$S_h = \frac{\rho_h}{\rho_c} \quad \text{(Eq. 29)}$$

$$K_P = 44.5\ w/(Mk) \quad \text{(Eq. 30)}$$

$$t_p = 0.001\ m \quad \text{(Eq. 31)}$$

$$D_i = 0.1\ m \quad \text{(Eq. 32)}$$

k_p is the thermal conductivity of the surface that separates the fluids. t_p is the thickness of the surface. D_i is the inner diameter of the spiral (Shirazi et al., 2022)

$$N = \frac{-D_i + (b_h - b_c)/2 + \sqrt{\left(D_i + (b_h - b_c)\right)^2 + (4L/\pi)(b_h + b_c + 2t_p)}}{b_h + b_c + 2t_p} \quad \text{(Eq. 33)}$$

N is the number of turns of the spiral.

$$A_{troca} = 2LH\ m^2 \quad \text{(Eq. 34)}$$

$$A_{cc} = b_c H\ m^2 \quad \text{(Eq. 35)}$$

$$A_{hc} = b_h H\ m^2 \quad \text{(Eq. 36)}$$

A_{troca} is the heat transfer area of the heat exchanger. A_{cc} and A_{hc} are the cross-sectional areas for the cold and hot fluids, respectively.

$$D_s = D_i + \left(b_h + t_p\right) + N(b_h + b_c + 2t_p) \quad \text{(Eq. 37)}$$

$$D_h = \frac{4Hb}{2(H+b)} \quad \text{(Eq. 38)}$$

D_s is the outer diameter of the spiral. D_h us the hydraulic diameter of the heat exchanger.

$$\varepsilon = \frac{D_h}{D_s} \quad \text{(Eq. 39)}$$

ε is the dimensionless parameter characteristic of the heat exchanger.

$$Re_h = 30000\ by\ definition \quad \textbf{(Eq. 40)}$$

Re_h is the maximum allowable Reynold number for the hot and cold fluids.

$$Re_{crit} = 20000\varepsilon^{0.32} \quad \textbf{(Eq. 41)}$$

Re_{crit} is the Reynolds number of transitions from laminar turbulent regime.

$$Re^* = \frac{Re_{nano}}{Re_h} \quad \textbf{(Eq. 42)}$$

Re_{nano} is the Reynold number associated with the nanofluid (Núñez et al., 2007; Shirazi et al., 2022).

$$h_h = \left[\frac{0.04\ Re_h^{0.74}\ Pr_h^{0.4}\ k_h}{D_h}\right](1 + 1.77\varepsilon)400 \leq Re_h \leq 30000 \quad \textbf{(Eq. 43)}$$

$$h_{nano} = \left[\frac{0.04\ Re_{nano}^{0.74}\ Pr_{nano}^{0.4}\ k_{nano}}{D_h}\right](1 + 1.77\varepsilon)400 \leq Re_{nano} \leq 30000 \quad \textbf{(Eq. 44)}$$

$$h^* = \frac{h_{nano}}{h_h} \quad \textbf{(Eq. 45)}$$

h_h and h_{nano} are the heat transfer coefficients of the hot and cold fluids, respectively. $(1 + 1.77\varepsilon)$ is the factor that considers the curvature of the spiral.

$$\dot{m}_h = \frac{\pi D_h \mu_h Re_h}{4} \quad \textbf{(Eq. 46)}$$

$$\dot{m}_{nano} = \frac{\pi D_h \mu_{nano} Re_{nano}}{4} \quad \textbf{(Eq. 47)}$$

$$\dot{m}^* = \frac{\dot{m}_{nano}}{\dot{m}_h} \quad \textbf{(Eq. 48)}$$

$\dot{m}_h$ and $\dot{m}_{nano}$ are the mass flow rates of the hot and cold fluids, respectively.

$$C_h = Cp_h \dot{m}_h \quad \textbf{(Eq. 49)}$$

$$C_{nano} = Cp_{nano} \dot{m}_{nano} \quad \textbf{(Eq. 50)}$$

C_h and C_{nano} are the heat capacities of the hot and cold fluids, respectively.

$$C^* = \frac{C_{min}}{C_{max}} \quad \textbf{(Eq. 51)}$$

C_{min} is the smallest of the fluid capacities.

$$U_0 = \frac{1}{\frac{1}{h_h}+\frac{t_p}{k_p}+\frac{1}{h_{nano}}} \quad \textbf{(Eq. 52)}$$

U_o is the overall heat transfer coefficient.

$$NTU = \frac{U_0\, A_{troca}}{C_{min}} \quad \textbf{(Eq. 53)}$$

NTU is the number of thermal units associated with heat exchanger.

$$Fa = \frac{NTU\ (1-C^*)}{2} \quad \textbf{(Eq. 54)}$$

Fa is the dimensionless number called the fin analogy.

$$\eta_T = \frac{Tanh(Fa)}{Fa} \quad \textbf{(Eq. 55)}$$

$$\varepsilon_T = \frac{1}{\frac{1}{\eta_T\, NTU}+\frac{(1+C^*)}{2}} \quad \textbf{(Eq. 56)}$$

η_T and ε_T are thermal efficiency and thermal effectiveness, respectively (Bejan, 1987; Fakheri, 2007).

$$\dot{Q} = \varepsilon_T C_{min}(Th_i - Tc_i) \quad \textbf{(Eq. 57)}$$

$$\dot{Q}_{max} = C_{min}(Th_i - Tc_i) \quad \textbf{(Eq. 58)}$$

$\dot{Q}$ is the heat transfer rate. Th_i and Tc_i are the inlet temperatures of the hot and cold fluids, respectively.

$$Tc_0 = Tc_i + \frac{\dot{Q}}{C_{nano}} \quad \textbf{(Eq. 59)}$$

$$Th_0 = Th_i - \frac{\dot{Q}}{C_h} \quad \textbf{(Eq. 60)}$$

$$T^* = \frac{Th_0 - Tc_i}{Th_i - Tc_i} \quad \textbf{(Eq. 61)}$$

$$\sigma_T = \frac{C_h}{C_{min}} \ln\left(\frac{Th_0}{th_i}\right) + \frac{C_{nano}}{C_{min}} \ln\left(\frac{Tc_0}{Tc_i}\right) \quad \textbf{(Eq. 62)}$$

$$\Delta P_c = \left(0.001\left(\frac{L}{S_{nano}}\right)\left(\frac{\dot{m}_{nano}}{D_s H}\right)\left[\frac{1.035\mu_{nano}^{1/2}}{D_s+0.125}\left(\frac{H}{\dot{m}_{nano}}\right)^{1/2} + 1.5 + \frac{16}{L}\right]\right) 10^4\ Re_{nano} < Re_{Crit} \quad \textbf{(Eq. 63)}$$

$$\Delta P_{nano} = \left(0.001\left(\frac{L}{S_{nano}}\right)\left(\frac{\dot{m}_{nano}}{D_s H}\right)^2\left[\frac{1.035\mu_{nano}^{1/3}}{D_s+0.125}\left(\frac{H}{\dot{m}_{nano}}\right)^{1/3}+1.5+\frac{16}{L}\right]\right)10^4 \; Re_{nano} > Re_{Crit} \quad \textbf{(Eq. 64)}$$

$$\Delta P_h = \left(0.001\left(\frac{L}{S_h}\right)\left(\frac{\dot{m}_h}{D_s H}\right)^2\left[\frac{1.035\mu_h^{1/3}}{D_s+0.125}\left(\frac{H}{\dot{m}_h}\right)^{1/3}+1.5+\frac{16}{L}\right]\right)10^4 \quad \textbf{(Eq. 65)}$$

ΔP_{nano} and ΔP_h are the pressure drops in the cold and hot fluids in the Pascal, respectively (Núñez et al., 2007; Shirazi et al., 2022).

$$P_{nano2} = P_{atm} \quad \textbf{(Eq. 66)}$$

$$P_{h2} = p_{atm} \quad \textbf{(Eq. 67)}$$

$$P_{nano1} = \Delta P_{nano} + P_{nano2} \quad \textbf{(Eq. 68)}$$

$$P_{h1} = \Delta P_h + P_{nano2} \quad \textbf{(Eq. 69)}$$

$$R = \frac{Th_i - Th_0}{Tc_0 - Tc_i} \quad \textbf{(Eq. 70)}$$

$$\sigma_f = -\frac{C_h}{C_{min}} R ln\left(\frac{P_{h2}}{P_{h1}}\right) - \frac{C_{nano}}{C_{min}} R ln\left(\frac{P_{c2}}{P_{c1}}\right) \quad \textbf{(Eq. 71)}$$

$$\sigma_T = -\frac{C_h}{C_{min}} ln\left(\frac{Ph_0}{Ph_i}\right) - \frac{C_{nano}}{C_{min}} ln\left(\frac{Pc_0}{Pc_i}\right) \quad \textbf{(Eq. 72)}$$

σ_T and σ_f are the thermal and viscous irreversibilities, respectively.

$$\dot{S}_{genT} = \sigma_T C_{min} \quad \textbf{(Eq. 73)}$$

$$\dot{S}_{genf} = \sigma_f C_{min} \quad \textbf{(Eq. 74)}$$

$\dot{S}_{genT}$ and $\dot{S}_{genf}$ are the thermal and viscous entropy generation rates, respectively.

$$Be = \frac{\dot{S}_{genT}}{\dot{S}_{genT} + \dot{S}_{genf}} \quad \textbf{(Eq. 75)}$$

Be is the Bejan number (Bejan, 1987; Fakheri, 2007; Ashrafizadeh, 2019).

3. RESULTS AND DISCUSSION

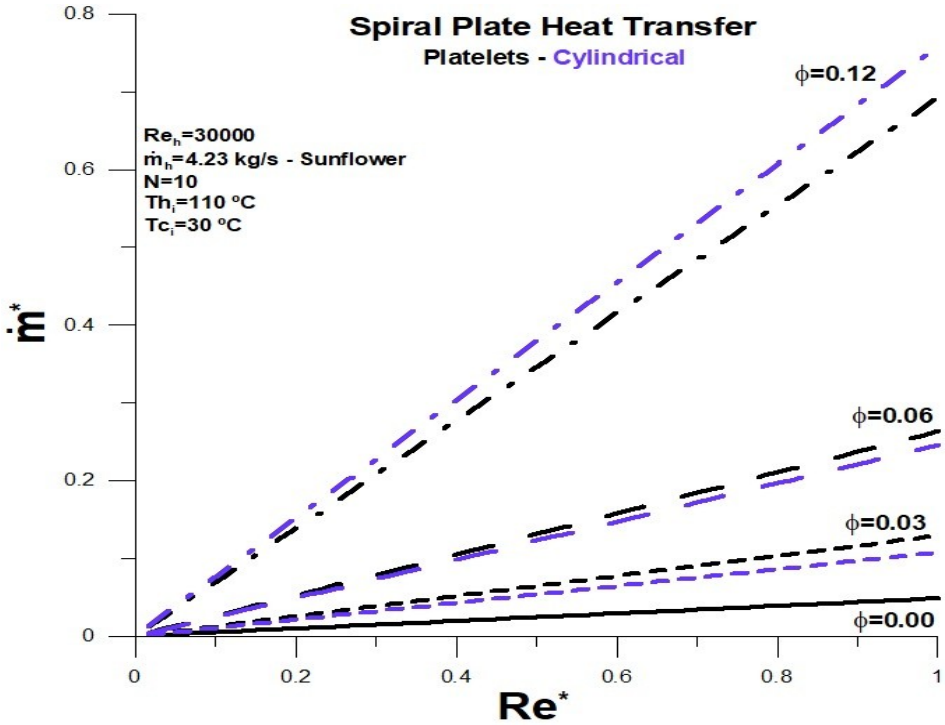

Figure 3. Dimensionless mass flow rate versus Reynolds number.

Fig. 3 presents results for the mass flow of refrigerant compared to the flow of hot fluid. The volume fraction of the nanoparticles ranges from 3.0% to 12.0%. The mass flow rate increases significantly when nanoparticles are added compared to the mass flow rate of pure water. There is no significant difference between the values obtained for the non-spherical nanoparticles analyzed. It can be predicted that the increase in mass should result in greater viscous dissipation, requiring greater power for the flow of nanofluid.

The two main quantities for determining the thermal efficiency of the heat exchanger are the ratio of the thermal capacities of the fluids (c*) and the number of thermal units (NTU). **Fig. 4** presents values for the relationship between the thermal capacities with volume fraction variation for the nanoparticles. The relationship between the thermal capacities grows with the increase in the refrigerant fluid flow, with a significant increase when the nanoparticles are added addition that will affect the thermal performance of the heat exchanger. A relevant fact is that, with the rise in the mass flow rate of the nanofluid, there is an exchange between the values of Cmin and Cmax; that is, the thermal capacity of the nanofluid exceeds the value of the thermal capacity of the hot fluid, when the volume fraction is equal to 12.0%.

The heat transfer coefficients associated with hot and cold fluids affect thermal performance and reflect variations in the number of thermal units (NTU). **Fig. 5** shows that the heat transfer coefficient of the cold fluid exceeds the transfer coefficient of the hot fluid when the flow rate of the cold fluid increases. This

increase is greater when nanoparticles are added, being on the order of three times greater for a volume fraction equal to 12.0%. For lower flow rates, the heat transfer coefficients associated with nanoparticles in the form of platelets are higher than the heat transfer coefficients for nanoparticles in the cylindrical shape. However, this trend is reversed for more significant fractions in volume.

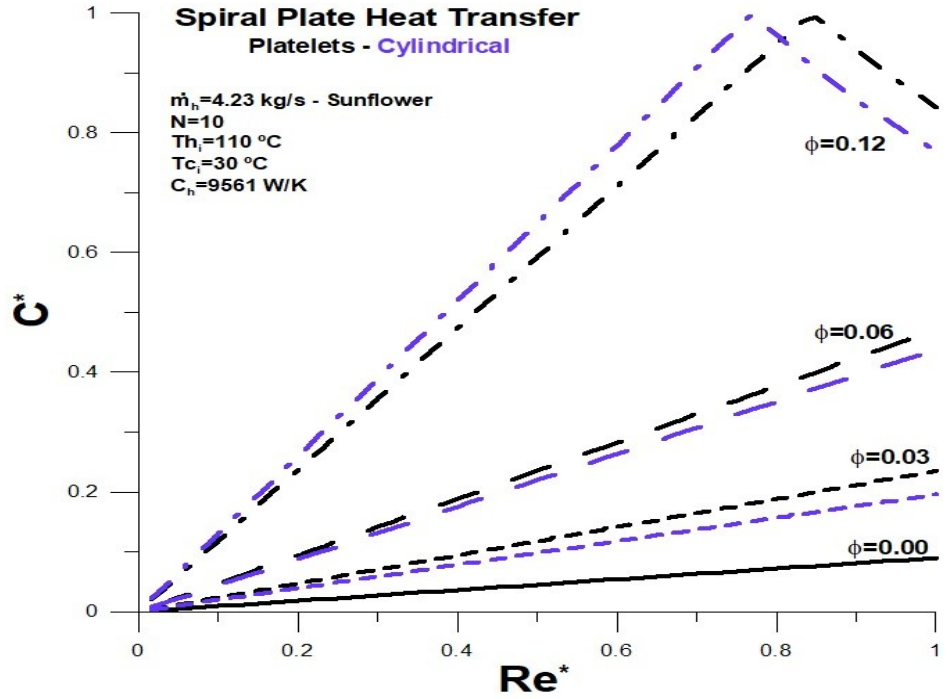

Figure 4. Relationship between heat capacities versus Reynolds number.

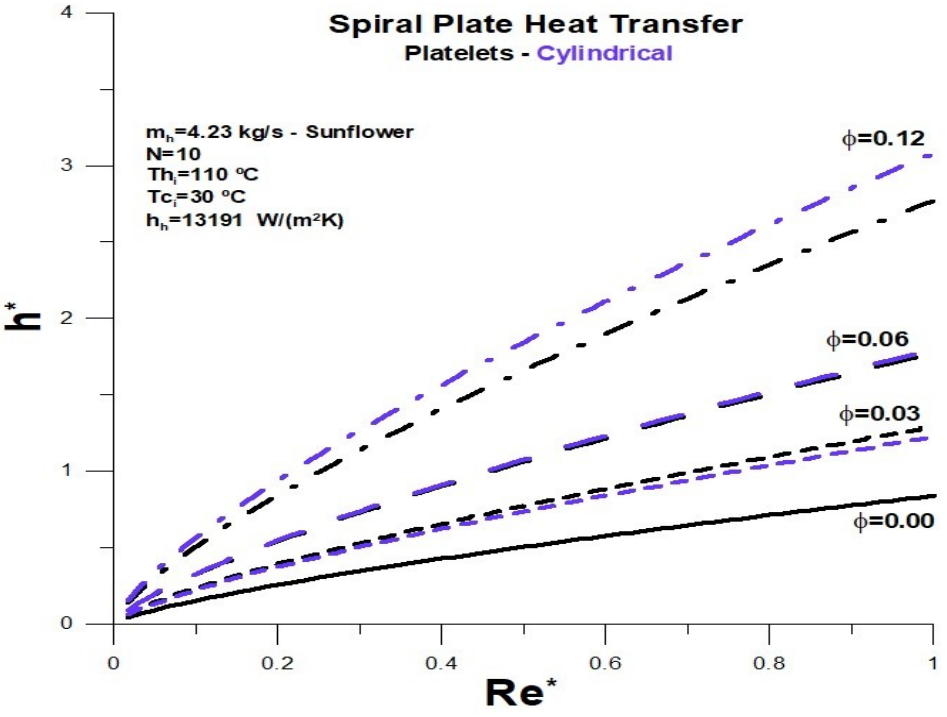

Figure 5. Relationship between heat transfer coefficients versus Reynolds number.

How to cite this article (APA): Nogueira, E. Analysis of Spiral Plate Heat Exchanger Used to Cool Vegetable Oil with Nanofluid Consisting of Water and Non-Spherical Boehmite Alumina Nanoparticles: Engineering & Technology Scientific Journal, 01(01), e023007.

Fig. 6 presents the number of thermal units associated with the current heat exchanger configuration. The number of thermal units decreases with increasing refrigerant flow rate. The decrease is greater when nanoparticles are added. For smaller volume fractions, the decline associated with nanoparticles in platelets is greater than that associated with nanoparticles in the cylindrical form. The situation is reversed with the increase in the volume fraction, reflecting what has already been observed for the heat transfer coefficients.

The thermal efficiency associated with the heat exchanger plays an essential role in the analysis, as the thermal effectiveness and the thermal irreversibility are defined. Fig. 7 presents results for thermal efficiency as a function of refrigerant flow. Efficiency grows with the increased inflow, and the increase is more significant with the rise in the volume fraction of the nanoparticles. In qualitative terms, the variation of the thermal efficiency is very similar to the variation of the ratio between the thermal capacities. From a maximum value, thermal efficiency equal to 1.0, there is a decrease with the increase in flow when the volume fraction is equal to 12.0%. The lower the efficiency value, the more effective the heat exchange between the fluids, indicating that the heat transfer rate is close to the maximum possible. In this case, the heat exchange potential has already been exhausted, and the difference between the fluid temperatures reached the lowest possible value in the situation under analysis. In contrast, a higher value for efficiency means that there is potential for heat exchange between fluids.

The thermal effectiveness, which measures the heat transfer rate concerning the maximum theoretically possible, is represented in Fig. 8. The result shows that for refrigerant fluid with a nanoparticle volume fraction lower than 12.0%, the heat exchange between the fluids reached its maximum value for the entire flow range under analysis.

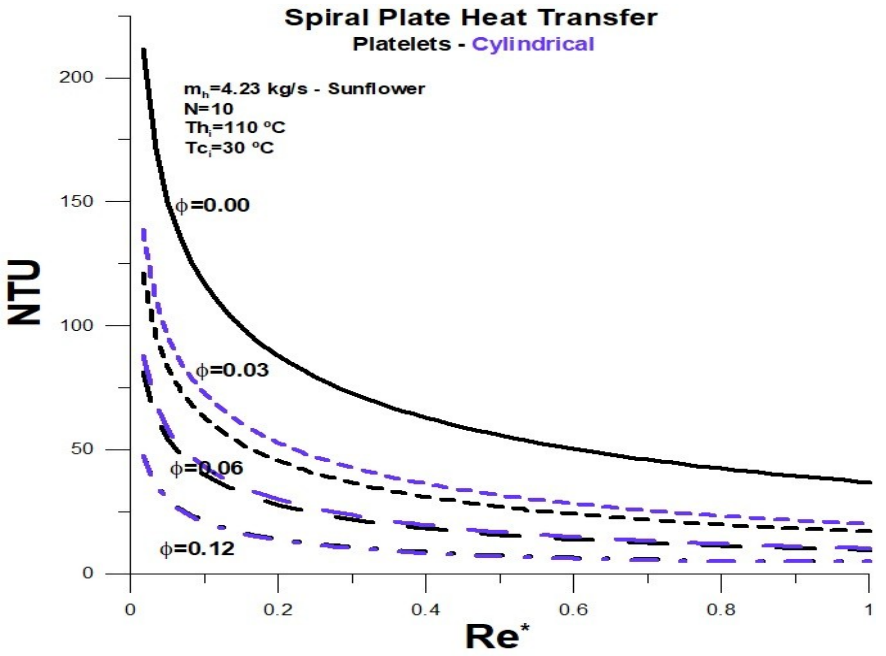

Figure 6. Number of thermal units (NTU) versus Reynolds number.

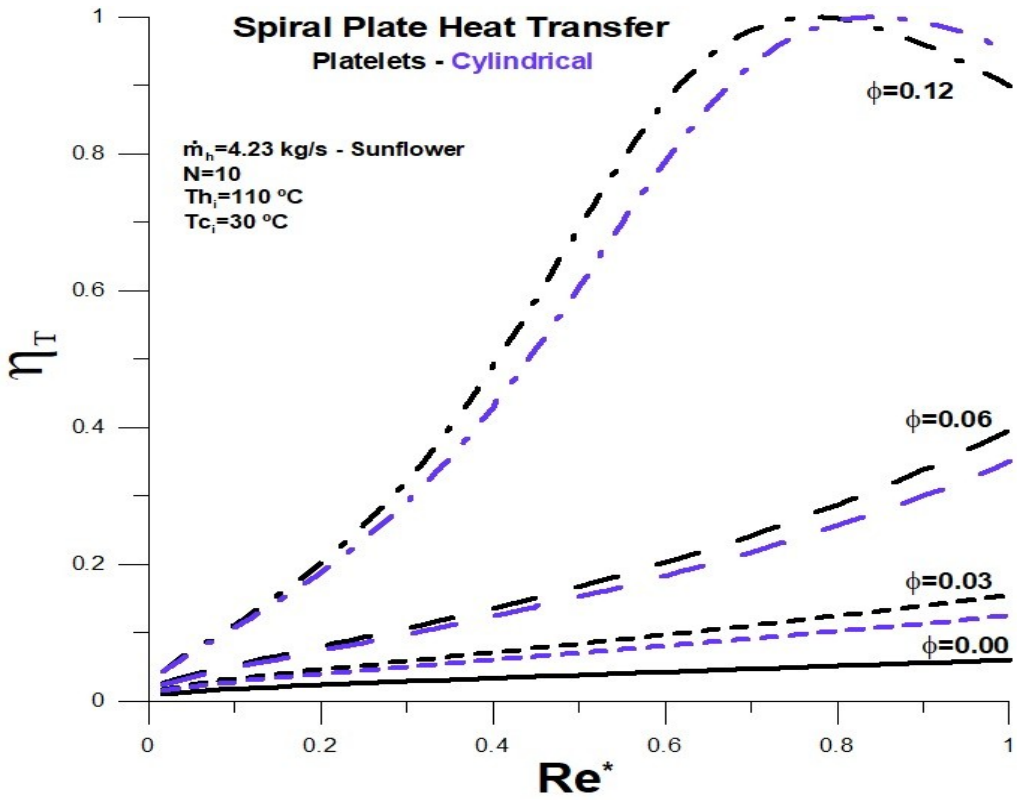

Figure 7. Thermal efficiency versus Reynolds number.

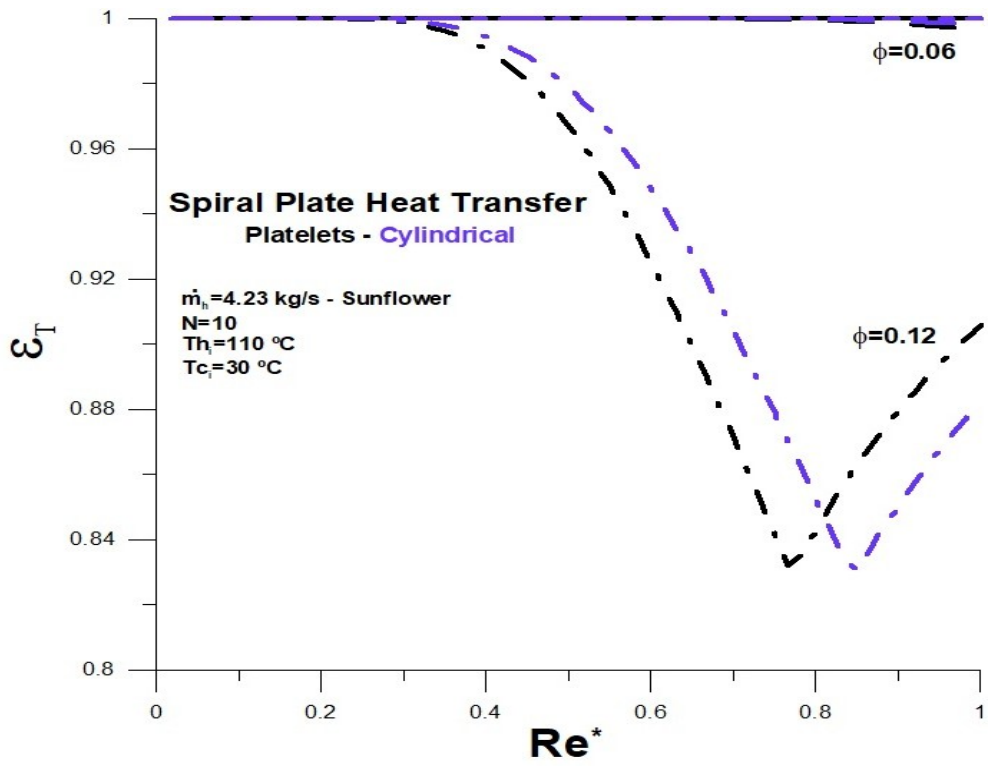

Figure 8. Thermal effectiveness versus Reynolds number.

For a volume fraction equal to 12.0%, it is shown that the heat transfer rate between the fluids is below the maximum possible and that a closer approximation occurs when there is an exchange of thermal capacity in determining the relationship between the thermal capacities.

Thermal irreversibility, **Fig. 9**, shows a similar trend to thermal effectiveness and in the opposite direction to thermal efficiency. However, the sensitivity to the effects of flow and volume fraction is greater than thermal effectiveness and very similar to thermal efficiency in qualitative terms, and vice versa. The greater the thermal irreversibility, the greater the probability that the heat exchange between the fluids has reached its maximum value and vice versa.

The viscous irreversibility, **Fig. 10**, measures the influence of viscous dissipation with the variation of the flow rate of the refrigerant fluid. The effect of viscous dissipation, when compared to the viscous dissipation of pure water, is relatively low for volume fractions less than 12.0%. However, when the volume fraction equals 12.0%, the viscous dissipation reaches relatively high values for Re*>0.6. This effect significantly weighs the cost-benefit ratio for the heat exchanger in the configuration under analysis. In addition, the power required for the flow to occur can be high.

The relationship between thermal irreversibility and total irreversibilities, the sum of irreversibilities, is associated with the Bejan number, **Fig. 11**. Viscous dissipation, represented by viscous irreversibility, is not significant for pure water, and thermal irreversibility is a predominant factor. When nanoparticles are added, viscous dissipation has a greater relative weight, around 40.0% for volume fractions

below and equal to 6.0%. For a volume fraction equal to 12.0%, it can be observed that the relative weight of viscous dissipation can reach the level of 80.0% when the flow of the refrigerant fluid approaches the flow of the hot fluid.

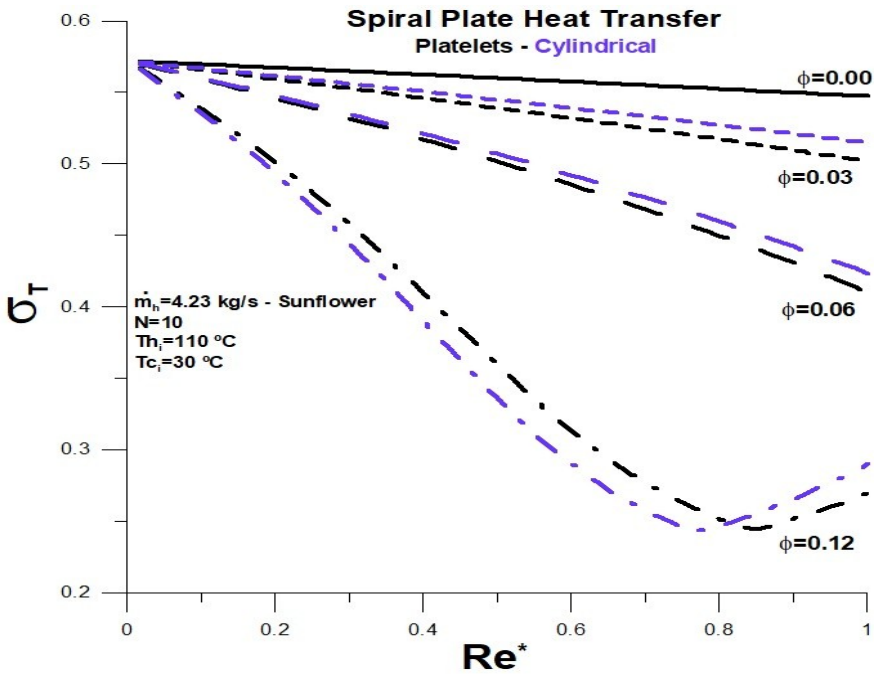

Figure 9. Thermal irreversibility versus Reynolds number.

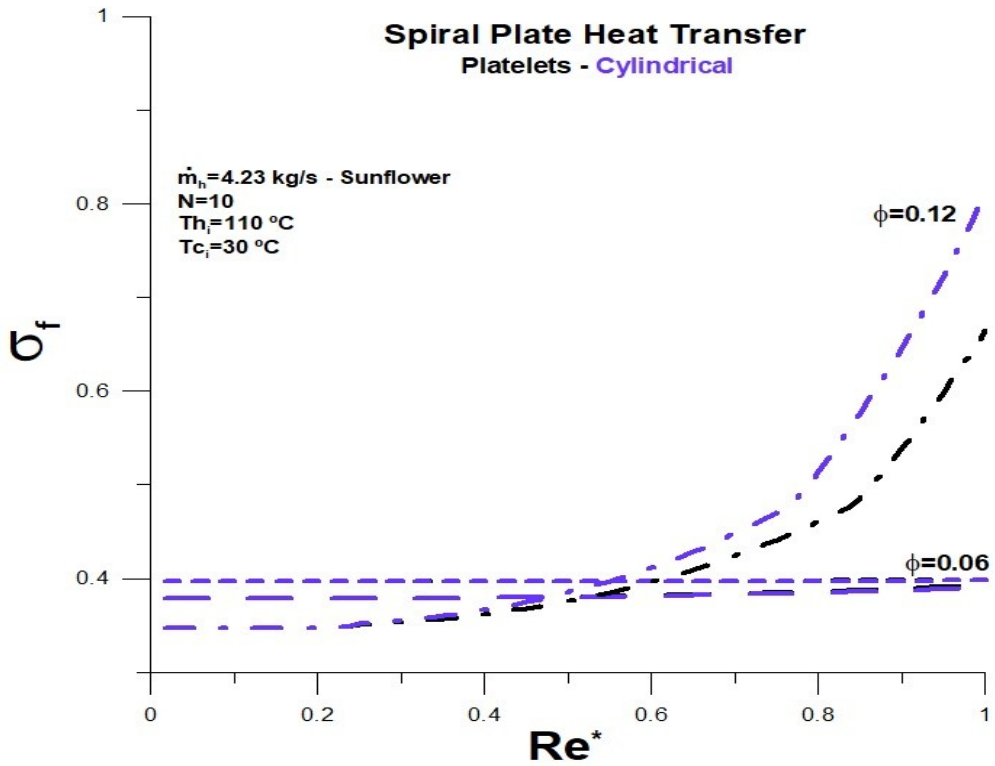

Figure 10. Viscous irreversibility versus Reynolds number.

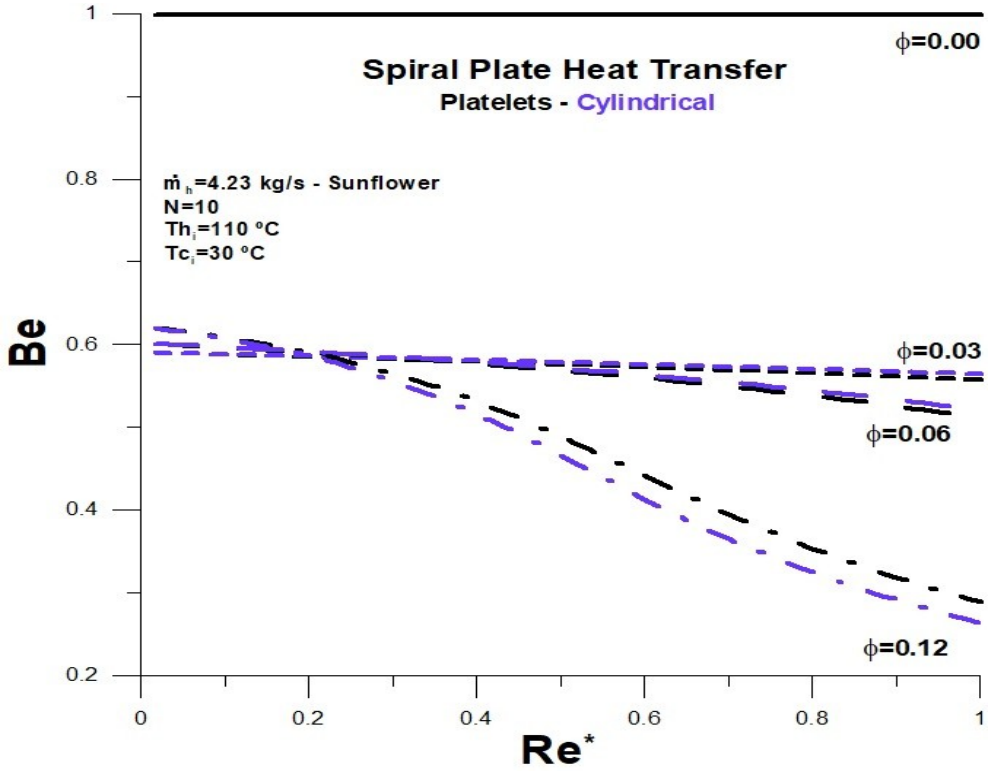

Figure 11. Bejan number versus Reynolds number.

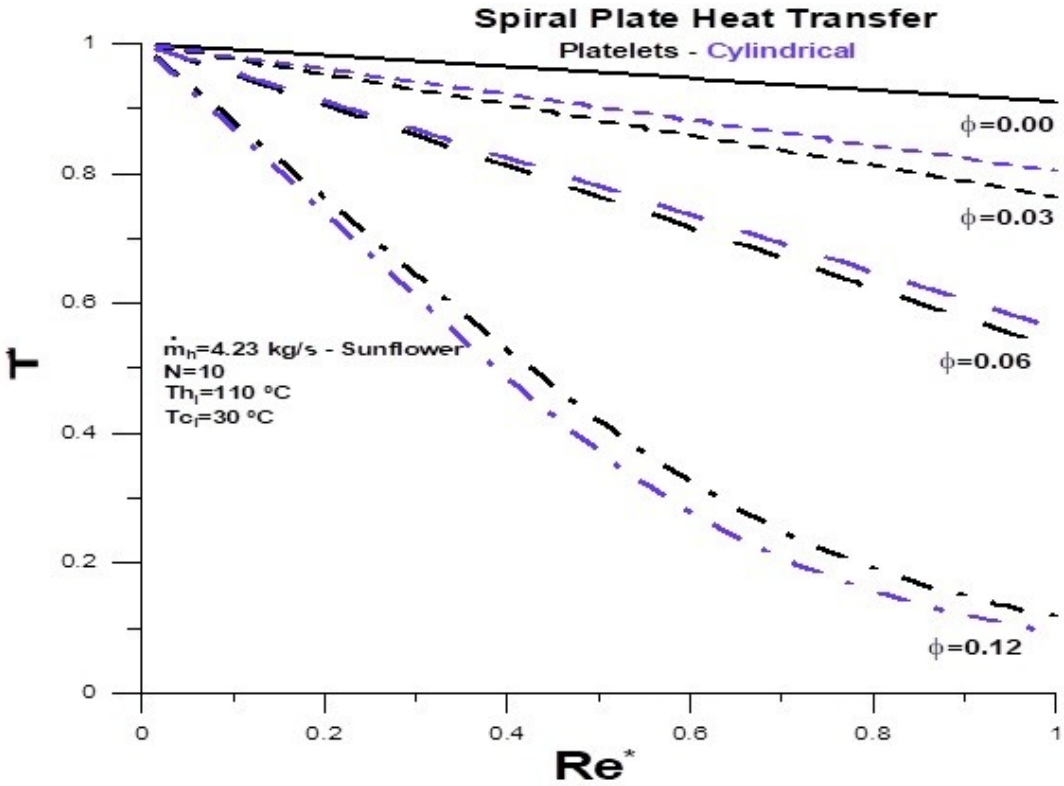

Figure 12. Hot fluid outlet temperature versus Reynolds number

The most important results related to the heat exchange are represented in Fig. 12 through the outlet temperature of the sunflower oil. Pure water has very little influence on the drop in temperature of the hot fluid in the entire flow range

analyzed. However, with the increase in the volume fraction, the temperature drop has accentuated values for both forms of nanoparticles. There is a more significant temperature drop for nanoparticles in the form of platelets, with a volume fraction below and equal to 6.0%. For volume fraction equal to 12.0%, the situation is reversed, but the temperature difference between both forms of nanoparticles is not significant. In the limiting condition under analysis, the lowest temperature of the hot fluid is approximately equal to 35.0 °C.

4. CONCLUSIONS

The influence of non-spherical Boehmite Alumina nanoparticles on the hydraulic and thermal performance of a spiral plate heat exchanger (S.P.H.E.) was analyzed. The formats of the analyzed nanoparticles are platelet and cylindrical. The fluid to be cooled is sunflower vegetable oil, and the base fluid is water, with an inlet temperature equal to 110.0 °C.

The thermal performance of the heat exchanger when using only pure water is poor, with a tiny drop in the temperature of the hot fluid. However, with the introduction of nanoparticles, added to the increase in the flow rate of the nanofluid, the temperature drop increases significantly. It achieves a better result for maximum flow within the flow rate under analysis. In this situation, with a volume fraction equal to 12.0%, the hot fluid outlet temperature reaches 35.0 °C.

It is concluded that the use of non-spherical nanoparticles provides excellent thermal performance, reflected in a lower outlet temperature of the hot fluid. By analyzing the Bejan number, it is possible to see that it is possible to increase the flow rate of the nanofluid in values slightly above what was studied or an increase in the volume fraction, which will reflect in a lower outlet temperature for the hot fluid. However, there will be an increase in viscous dissipation, compromising the cost-benefit ratio.

5. AUTHOR INFORMATION

Élcio Nogueira
e-mail address: elcionogueira@outlook.com

REFERENCES

Ashrafizadeh, S. A. (2019). Application of Second Law Analysis in Heat Exchanger Systems. *Entropy*, *21*(6), 606. https://doi.org/10.3390/e21060606

B. Hemanth, K. Prasada Rao, & S. Venkateswara Rao. (2022). Heat Transfer Enhancement in Spiral Plate Heat Exchanger Using Nanofluids. *International Journal of Creative Research Thoughts (I.J.C.R.T.)*, *10*.

Bejan, A. (1987). The thermodynamic design of heat and mass transfer processes and devices. *International Journal of Heat and Fluid Flow*, *8*(4), 258–276. https://doi.org/10.1016/0142-727X(87)90062-2

Fakheri, A. (2007). Heat Exchanger Efficiency. *Journal of Heat Transfer*, *129*(9), 1268–1276. https://doi.org/10.1115/1.2739620

K. Pradeep Mohan Kumar, V. Vijayan, B. Suresh Kumar, C. M. Vivek, & S. Dinesh. (2018). Computational Analysis and Optimization of Spiral Plate Heat Exchanger. *Journal of Applied Fluid Mechanics*, *11*(SI). https://doi.org/10.36884/jafm.11.SI.29428

Khorshidi, J., & Heidari, S. (2016). Design and Construction of a Spiral Heat Exchanger. *Advances in Chemical Engineering and Science*, *06*(02), 201–208. https://doi.org/10.4236/aces.2016.62021

Kolasiński, P., & Rogala, Z. (2015). The use of spiral heat exchangers in the orc domestic systems. *Scientific Letters of University of Rzeszow Technology - Mechanics*, *32*(87(1/2015)), 23–35. https://doi.org/10.7862/rm.2015.3

Nogueira, E. (2020). Thermal Performance in Heat Exchangers by the Irreversibility, Effectiveness, and Efficiency Concepts Using Nanofluids. *Journal of Engineering Sciences*, *7*(2), F1–F7. https://doi.org/10.21272/jes.2020.7(2).f1

Picón Núñez, M., Dávalos, L. C., & Fuentes, A. M. (2007). *Alternative design approach for spiral plate heat exchangers*.

Rojas, E. E. G., Coimbra, J. S. R., & Telis-Romero, J. (2013). Thermophysical Properties of Cotton, Canola, Sunflower and Soybean Oils as a Function of Temperature. *International Journal of Food Properties*, *16*(7), 1620–1629. https://doi.org/10.1080/10942912.2011.604889

Sabouri Shirazi, A. H., Ghodrat, M., & Behnia, M. (2022). Energy and exergy analysis of spiral turns in optimum design spiral plate heat exchangers. *Heat Transfer*, *51*(1), 701–732. https://doi.org/10.1002/htj.22326